WATER
WATER
WATER
WATER
WATER
WATER
WATER
WATER
WATER
WATER

Project Completion
Report No. 712508

A REMOTE SENSING TECHNIQUE FOR ESTIMATING WATERSHED RUNOFF

Olin Mintzer
Farid Askari
Department of Civil Engineering
The Ohio State University

United States
Department of the Interior

Contract No.
A-063-OHIO

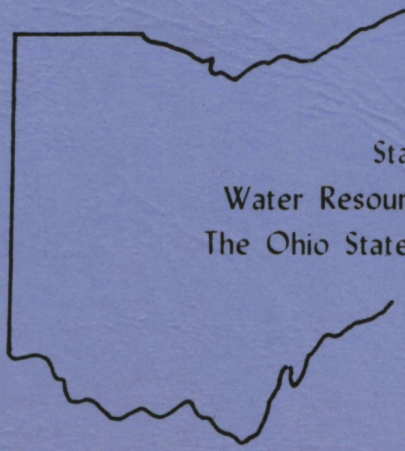

State of Ohio
Water Resources Center
The Ohio State University

A REMOTE SENSING TECHNIQUE FOR ESTIMATING WATERSHED RUNOFF

by

Olin Mintzer
and
Farid Askari

Civil Engineering Department
The Ohio State University

WATER RESOURCES CENTER
Engineering Experiment Station
The Ohio State University

October 1980

This study was supported in part by the
Office of Water Research and Technology,
U. S. Department of the Interior under
Project A-063-OHIO

LIST OF FIGURES

LIST OF TABLES

INTRODUCTION

Background

Effective watershed management requires the ability to predict runoff A wide range of empirical formulas for predicting peak runoff for Ohio watersheds have already been investigated. For the unglaciated uplands of southeastern Ohio; the most satisfactory results were obtained from Chow runoff formulas. The key input to the Chow formula comes from the parameters that describe the watershed's surface characteristics in terms of land surface cover conditions and soil types as shown in Table 1. From these parameters a runoff coefficient (CN) is selected. The data for the formula comes from topographic maps, aerial photos, and field visits to all parts of the watershed.

A promising technique for determination of these land cover parameters involves the use of computer-aided analysis of remotely sensed data. Spatial-temporal observations obtained from remotely sensed techniques contain specific information useful in assessing both the water quantity and quality parameters.

The utility of remote sensing data in land cover classification has been demonstrated in earlier investigations. (Sasso, 1977; Ragan, 1975). However, in all the studies reviewed the successful methodologies have involved the extraction of only land cover(leyel I) information from LANDSAT multi-spectral data on a regional basis. Detailed surface condition information provides a better representation of the spatial variability of surface runoff; thus effective land management practices may be established to control peak flow and water yield from the watersheds. The technique and its application are treated in this report.

Objective

It is the objective of this investigation to derive the runoff coefficients for watersheds from the LANDSAT multi-spectral data by including the more detailed (level II) surface conditions and soil types along with land cover (level I) types in the analysis techniques.

Table 1. Chow's Land Cover Parameters Modified for Mill Creek Watershed.

Land Cover Level I	Surface Conditions Level II	Runoff Coefficient (CN) Soil Type B	C
Fallow	straight row	86	91
Row Crop (Corn)	straight row	80	87
	contoured	77	83
	contoured and terraced	73	79
Pasture and Grassland	poor	79	86
	normal	69	79
	good	61	74
Farm Woodlots	sparse	66	77
	normal	60	73
	dense	55	70
Impervious Surface		100	100

SUMMARY

The multi-spectral data from LANDSAT were used in combination with aircraft color infrared photography to derive the runoff coefficients for the watersheds of Mill Creek, Coshocton County, Ohio.

Regression models were developed from treating the runoff coefficient of each sample site as the dependent variable and the mean radiance measurements in the four LANDSAT channels as the independent variables. The models were then extended over the area, and the results of the classification consisted of digital color-coded maps illustrating the spatial variability of runoff potential for the surface. The computer-derived patterns were confirmed with the known features within the area. Individual test fields and test watersheds were selected for verification of the model results. The mean runoff coefficients derived from the models compared favorably with those obtained from ground truth.

For the sampled sites of the given land cover conditions and soil type, the multi-spectral data analysis technique provided reasonable values of coefficients for the watersheds tested.

MATERIALS AND METHODS

For this investigation a stepwise data acquisition procedure integrated topographic, geologic, soils and vegetation data and ground truth data from low altitude color infrared photography with multi-spectral data from one scene each of LANDSAT-2 and LANDSAT 3.

To facilitate the assignment of runoff coeffiecients, an index for run-off was adopted based on the criteria of soil cover complex (CHOW and SCS, 1962); the coefficients were related to the land cover, surface condition and hydrologic soil group as shown in Table 1.

Location and Characteristics of the Study Area

The Mill Creek Watershed, with an approximate area of 17000 acres located at latitude $40^{o}22'$N and longitude $81^{o}48'$W in Coshocton County, Ohio, was selected for testing in this investigation. The choice of the study area included the following considerations. First, the general characteristics of the study watershed were representative of most of the agricultural-forested uplands lying to the northwest of the Appalachian plateau. Second, current and historical data concerning the geology, land use and hydrology existed for the watershed. Third, the proximity of the watershed to the USDA Agricultural Experiment Station was convenient. And finally, the effects of soils, land management, geology and climate on water flow from the agricultural land were known.

The site is characterized by bench-like topography resulting from differential weathering of interbedded hard and soft layers of sandstone and shale, with minor interbedding planes of clay, coal and limestone. The western half of the elliptical watershed is drained by Mill Creek, which flows north to south. The lower eastern half is drained by Little Mill Creek; the flow and confluence of these creeks within the watersheds form a dendritic to sub-dendritic drainage pattern.

Data Acquisition

The first step was to determine the hydrologic characteristics of the various soils within the watersheds. By compiling the information obtained from the soils map (USDA, Soil Survey for Little Mill Creek), the 1:24000 topo maps, and the USGS quad-centered photography, the watershed was classified into three well-delineated terrain regions. A base map illustrating the spatial characteristics for the regions was constructed at the scale of 1:24000. The soil group associated with the uplands and colluvial slope

Table 2. Terrain-Soil Groups

Terrain regions	Hydrologic soil group
uplands	B
colluvial soils	B
filled valleys	C

regions consisted of predominantly coarse-textured sands and sandy loams. The runoff potential for both regions was expected to be low, due to the occurrence of pervious caprocks and coarse-textured soils and contour-terraced and wooded slopes.

The characteristic elements associated with the filled valleys and drainage ways that were designated as having high potential for runoff consisted of soils containing fine-textured silts, silty loams and clays, straight row crops and seepage water from the base of slopes.

Positive color infrared transparencies, flown for this project on September 20, 1979, at the scale of 1: 24000, were used as the primary source of ground truth in support of the LANDSAT data. LANDSAT imagery for May 6 and June 20, 1979 for the area of interest was found to be free of cloud cover. The land cover surface condition at the time of the May 6th LANDSAT scene was assumed to consist of fallow agricultural fields, pasture and small woodlots.

The data from the June 20th scene represented the growing season, in particular, the time when the agricultural fields were under cultivation. The method used to differentiate the surface conditions was based on the textural variations from field-to-field. For example, distinct textural differences were discernable for woodlots of sparse canopy versus dense canopy, or straight row crops versus contoured row crops. Finally, the results of the interpretation were transferred to a base map at the 1:24000 scale.

Representative sample sites describing the variability of the watershed surface were selected from the existing base maps. Guidance from Table 1 and the soils and vegetation base maps provided a runoff coefficient (CN) assignment for each sample site. See Appendix A for lists of training samples.

DATA ANALYSIS

In the analysis the digital (magnetic) tapes produced from LANDSAT were used to extrapolate the runoff information over the entire study area by computer manipulation. The raw data from the computer compatible tapes (CCT's) of LANDSAT represented the reflected radiant energy from land surface features. The data were recorded in two visible and two near infrared portions of the spectrum.

Discriminant models based on the relationship between the runoff coefficients (CN values) and the radiance measurements were developed. The analysis procedure follows. First the raw multi-spectral (CCT) data were displayed on a color image processing unit. By manual overlay the preselected ground sample sites were located and registered based on the spectral uniformity. For each sample site (a block of 3 x 3 pixels) four separate mean radiance values (one value for each LANDSAT channel) were computed from statistical analysis. These average radiance sample values were used as the four independent variables, and runoff coefficients were assigned from ground

truth as the dependent variables for a series of regression models of the following form:

$$CN = B_0 + B_1 x_4^{\alpha} + B_2 x_5^{\alpha} + B_3 x_6^{\alpha} + B_4 x_7^{\alpha}$$

For both LANDSAT scenes a design matrix of radiance versus runoff coefficients was constructed, and the CN values were plotted against the individual channels in order to observe the nature of dispersion of the data in the four dimensional space.

RESULTS AND DISCUSSION

The coefficient of correlation between the dependent and the independent variables was used to evaluate the significance of each variable. Using standard regression techniques, a number of linear and polynomial regression models were tested for each data set, and the optimum set of exponents and coefficients that produced the best fit were selected. The best fit was evaluated in terms of the R^2, the measure of closeness with which the radiance variables described the runoff coefficients.

For the May 6th data, the relationship between the channel radiance and the runoff coefficient is explained better in terms of a polynomial rather than a linear model. The "F" values for each variable in the model are recorded in Appendix D, and all the values are realistic at the 0.05 level of significance.

May 6, 1979 LANDSAT Data

$$CN = B_0 + B_1 X_4 + B_2 X_5^{1/3} + B_3 X_6^{-\frac{1}{2}} + B_4 X_7^{-1/3}$$

CN = runoff coefficient

X_4 = the mean radiance value for channel 4

X_5 = the mean radiance value for channel 5

X_6 = the mean radiance value for channel 6

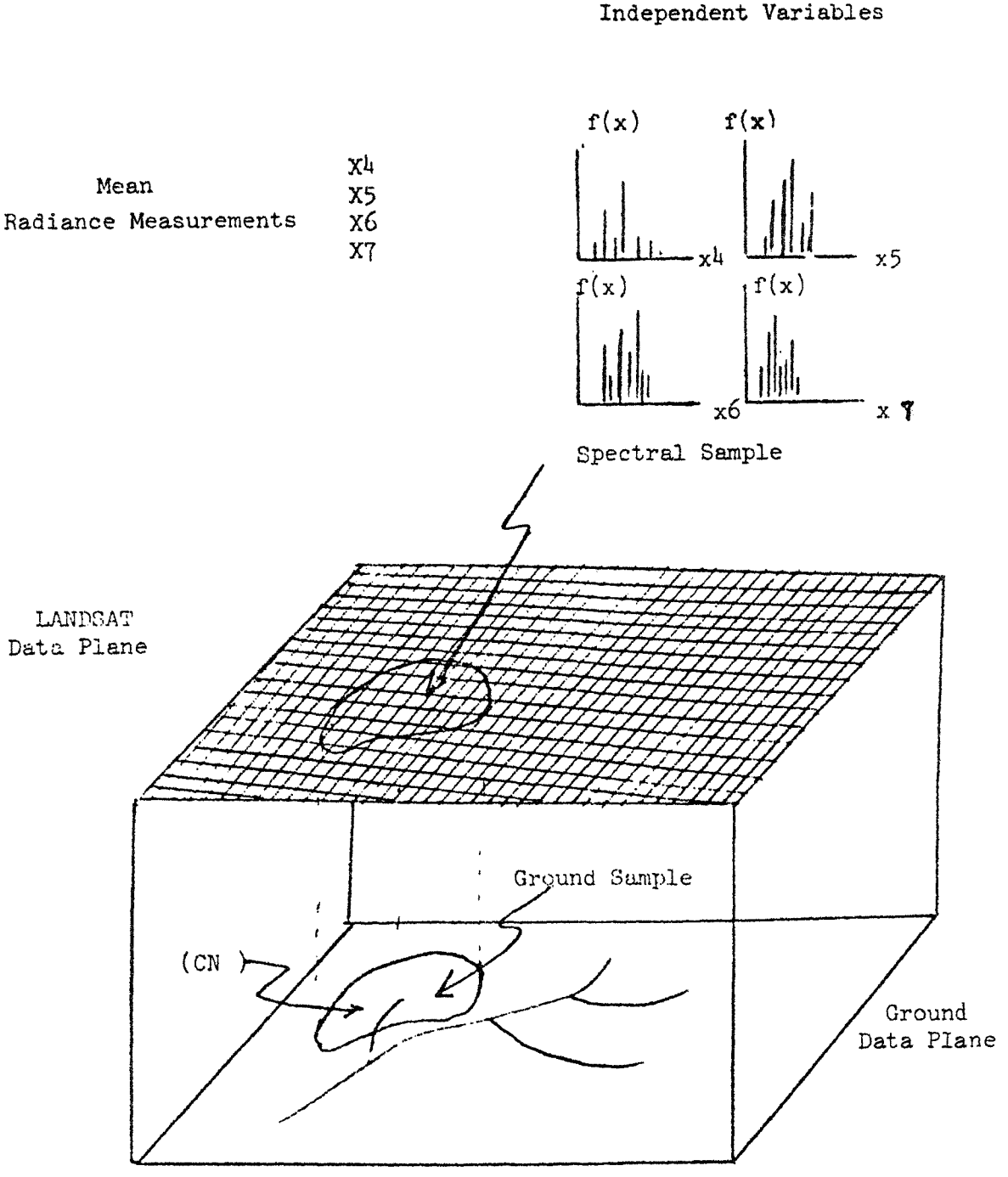

FIGURE 1. Stratified Data Plane for CN-Radiance Samples

X_7 = the mean radiance value for channel 7

$B_0 = 13.71, B_1 = 4.70, B_2 = 54.61, B_3 = 2308.9, B_4 = 1330.3$

For the June 20th data, only a linear model produced significant results. Because of the high correlations between the pair of visible and infrared channels, it was decided to use only two channels (one visible and one infrared). For this particular model only channel 5 was significant at the 0.05 percent level.

June 20, 1979 LANDSAT Data

$CN = B_0 + B_1X_5 + B_2X_7$

CN = runoff coefficient

X_5 = the mean radiance for channel 5

X_7 = the mean radiance for channel 7

$B_0 = 72.56$, $B_1 = 0.32$, $B_2 = -0.06$

The exponents and coefficients for other models appear in Appendix E.

Each regression model was extended over the study area, and based on the radiance values a CN value was assigned to each pixel. The final products resulting from the discrimination process were two color-coded digital maps showing the spatial distribution of runoff potential (CN) for the watershed surface. A typical color-coded product, Figure 2, was derived from the computer analysis of the May 6 LANDSAT data. The color patterns correspond from lower CN to higher CN runoff coefficients increasing in accordance with the following sequence of colors:
dark blue, blue, dark green, green, yellow, orange, brown, red, dark red. The analysis of patterns are confirmed with the known features within the area. For example, in Figure 2, the natural drainage system appears to be in the range of CN of 90 to 100, which is consistent with the fact that the earliest response of the watershed to a storm is associated with the drainage

Color	CN
dark blue	90
blue	91
dark green	92
green	93
yellow	94
orange	95
brown	96
dark red	97
red	98
dark purple	100

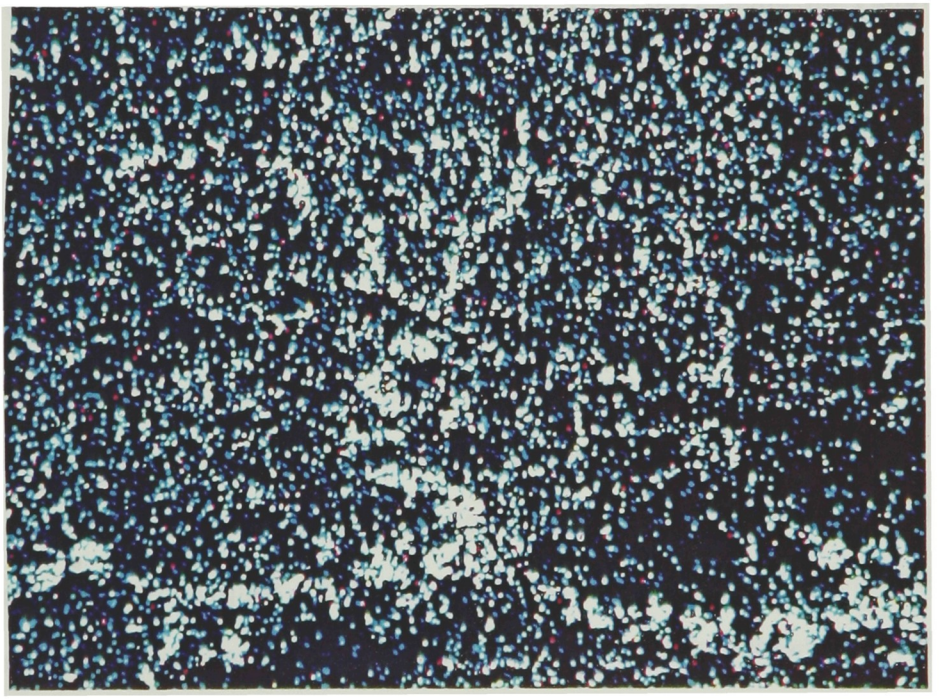

Figure 2 The Spatial Distribution of CN, Runoff Coefficients for the Area, May 6, 1979

system. Also, the river surfaces are consistently registering as regions of 100 percent runoff. (For other values of CN, 90 or less, reference is made to Askari, 1980.)

Figure 3 shows the same range of runoff coefficients for the area acquired from the June.20th LANDSAT scene. The temporal comparison illustrates the change in the spatial distribution of runoff potential for the surface. The average runoff predicted for the study area decreased from May to June;this would be expected due to an increase in the land cover and foliage on the surface.

To assess classification performance of the models, small test watersheds of the Little Mill Creek, shown in Figure 4, located in the lower southeast quadrant of the Mill Creek, were selected for analysis. For each test watershed (see Figure 4) a weighted runoff coefficient was calculated using the area ratio of each soil cover complex and the corresponding runoff coefficients.

A number of single cover test fields with known runoff conditions also were chosen from different locations within the watershed. From an overlay of topographic maps, boundaries for the individual test watersheds were extracted and correlated with the initial spectral data. Using the statistical analysis programs, the mean radiance values for the test sub-watersheds and test fields were calculated and supplied to the regression models.

In predicting the mean CN values for the test watersheds from multispectral analysis techniques, the models performed well. Disagreement was apparent for two sub-watersheds, 13 and 91, where both sub-watersheds consisted of one single land cover,compared to the other watersheds that contained a mixture of land covers. For the individual test fields, the models constructed for the June data produced better results (See Appendix E, tables 1 and 2).

Color	CN
dark blue	90
blue	91
dark green	92
green	93
yellow	94
orange	95
brown	96
dark red	97
red	98
dark purple	100

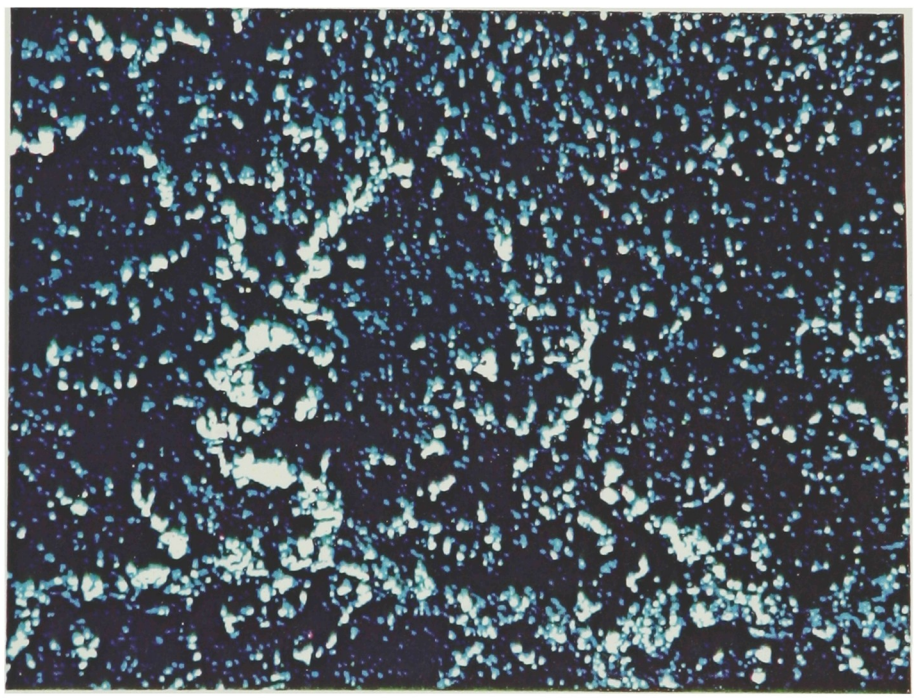

Figure 3 The Spatial Distribution of CN, Runoff Coefficients for the Area, June 20, 1979

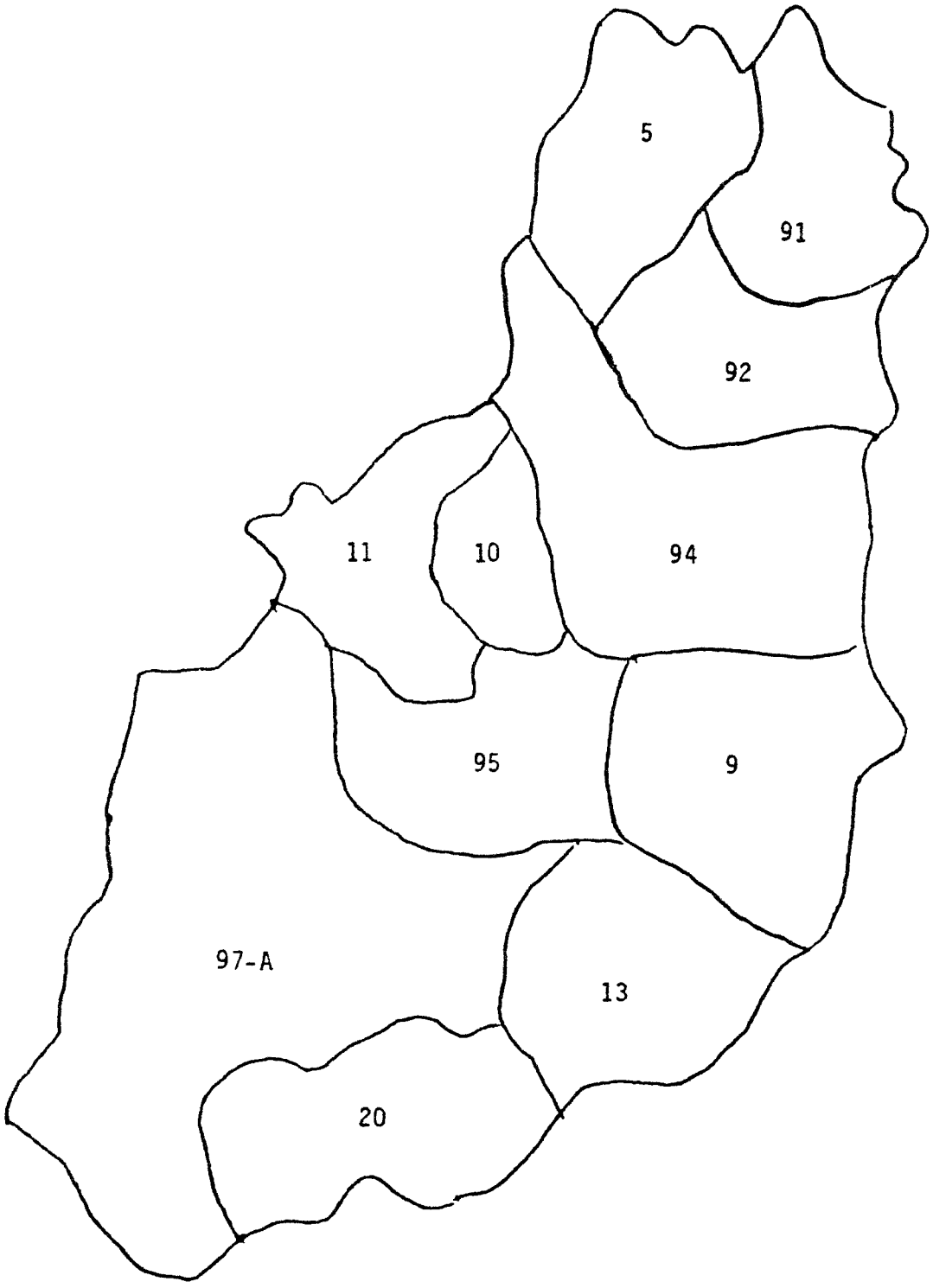

FIGURE 4 Location of Test Watersheds in the Little Mill Creek

In general, the results were more promising for a combination of fields or watersheds rather than the individual fields. Appendix F (Tables 1, 2, and 3) shows the accuracy resultant from an analysis of LANDSAT multi-spectral data versus the ground truth information. The weighted CN values for the watersheds provided from the June 20th data compared more favorably with the ground truth than that of the unweighted data (see Appendix F, Table 3).

CONCLUSIONS

The results of this investigation were encouraging, and the work performed in the study demonstrated a step toward providing detailed information for hydrological studies from LANDSAT data. Based on the evaluation of the technique and results of the models used, the following conclusions are summarized.

1. The processing technique implemented for the intergrated use of aircraft data and LANDSAT data differed significantly from the traditional methods of hydrologic land cover classification in the sense that the surface conditions and soil types for a particular land cover were incorporated in the spectral-classification procedure.

2. The derivation of the regession models were scene and ground truth dependent.

3. The regression models performed very well in predicting the weighted (CN) values for subwatersheds.

4. With a known boundary for a subwatershed, the extraction of the weighted CN vs. the mean radiance value of a given spectral channel were independent of the identity of land cover-surface condition, and the results were based only on the spectral response of the given subwatershed.

5. The color-coded visual display provides a good means for defining the spatial variability of the watershed's runoff coefficients.

6. The results obtained from the regression models, incorporated the surface conditions (level II) successfully to provide watershed runoff coefficients from LANDSAT data.

RECOMMENDATIONS

There are several aspects in the analysis and the development of the technique that need to be examined further in future work with LANDSAT. It is recommended that:

1. The size of the design matrix (number of observations) be increased.

2. Examination of various types of regression models be made.

3. Accounting be made of the weighting of the coefficient and the exponent of the slope variable in the regression model.

4. An alternative sampling scheme be used involving varying sample sizes and assigning weights to those samples that are hydrologically more significant.

5. Data registration be made with multi-spectral data to include the ancillary data being digitized (soil boundaries, vegetation, geology) forming one common geographic reference system.

6. Use be made of the digital terrain data based on USGS 1/250,000 scale topographic maps which are readily available from the National Cartographic Information Center.

REFERENCES

1. Askari, F., 1980, "Automated Classification of Watershed Runoff Coefficients from LANDSAT Multispectral Data," A Thesis Presented in Partial Fulfillment of Requirements for Master of Science Degree, The Ohio State University, Columbus, Ohio.

2. Barr, B. C., 1979, "Statistical Analysis System" SAS Institute Incorporated, Raleigh, N.C.

3. Baumgardner, E. R., Cipra, J. E., 1971, "Measuring Radiance Characteristics of Soil with a Field Spectroradiometer," Proceedings of the American Soil Science Society.

4. Blanchard, B. J., 1975, "Remote Sensing Techniques for Prediction of Watershed Runoff," Proceedings of the NASA Earth Resources Survey Symposium, Volume 1-D, Water Resources Section.

5. Chow, V. T., 1962, "Hydrologic Determination of Waterway Areas for the Design of Drainage Structures in Small Drainage Basins," University of Illinois Bulletin No. 462.

6. Estes, J. E., Hooper, J. O., 1977, "Measuring Soil Moisture with an Airborne Imaging Passive Microwave Radiometer," Photogrammetric Engineering and Remote Sensing, Vol. 43, No. 10.

7. Gates, D. M., 1970, "Remote Sensing with Special Reference to Agriculture and Forestry," National Academy of Sciences, Washington, D.C.

8. Graves, D. H., 1975, "Remote Sensing of Effects of Land-Use Practices on Water Quality," Kentucky University, National Technical Information Service, Accession Number CR-144105.

9. Jurica, G. M., Murray, W. L., 1972, "Influence of Haze Layers on Remotely Sensed Surface Properties," LARS Print Number 060272, Purdue University.

10. Kelley, G. E., "Soils of the North Appalachian Experimental Watershed," U.S. Department of Agriculture, Report No. 1296.

11. Khorram, S., 1979, "Remote Sensing Analysis of Water Quality in the San Francisco Bay-Delta," Proceedings of the Thirteenth International Symposium on Remote Sensing of Environment, ERIM, Michigan.

12. Khorram, S., 1979, "Use of Landsat and Environmental Satellite Data in Evapotranspiration Estimation from a Wild Land Area," Proceedings of the Thirteenth International Symposium on Remote Sensing of Environment, ERIM, Michigan.

13. Kristof, S. J., Baumgardner, M. F., Johannsen, C. J., 1973, "Spectral Mapping of Soil Organic Matter," LARS Information Note 030773, Purdue University.

14. Kumar, R., 1972, "Radiation from Plants - Reflection and Emission: A Review," Research Project No. 5543, Purdue Research Foundation.

15. Lindelaub, J. C., Cary, T. K., 1975, "A Case Study Using LARSYS for Analysis of Landsat Data," LARS Information Note 050575, Purdue University.

16. Morgan, K. M., Lee, G. B., 1978, "Prediction of Soil Loss on Cropland with Remote Sensing," Texas Christian University, Journal of Soil and Water Conservation, Vol. 13, Nov.-Dec. issue.

17. Murray, W. L., Jurica, G. M., 1973, "The Atmospheric Effect in Remote Sensing of Earth Surface Reflectivities," LARS Information Note 110270, Purdue University.

18. Owen, S. M., 1970, "Modification of the Stanford Watershed Model to Improve Groundwater Simulation for Stratified Geologic Regions," M.S. Thesis, Civil Engineering, The Ohio State University.

19. Olsen, D. E., 1961, "Seasonal Changes in Light Reflectance From Forest Vegetation," Photogrammetry Engineering, Vol. 27, No. 1.

20. Orlov, D. S., 1966, "Quantitative Patterns of Light Reflection on Soils," Soil Science No. 13 Supplement.

21. Pickens, J. B., 1977, "Application of Selected Runoff Formulas to Stark County, Ohio Watersheds," M.S. Thesis, Civil Engineering, The Ohio State University.

22. Pitts, D. E., McAllum, W. E., 1977, "The Effect of Atmospheric Water Vapor on Automatic Classification of ERTS Data," Proceedings of the Eleventh International Symposium on Remote Sensing of Environment, ERIM, Michigan.

23. Potter, W. D., Baker, M.V., 1930, "Some of the Factors Influencing the Behavior of Perched Water-Tables at the North Appalachian Experimental Watershed Near Coshocton, Ohio," Hydrology Lab, The Ohio State University.

24. Ragan, R. M., Jackson, T. J., 1975, "Land Use Classification for Hydrologic Models Using Interactive Machine Classification of Landsat Data," Proceedings of the NASA Earth Resources Survey Symposium, Vol. 1-D, Water Resources.

25. Rango, A., Salomonson, V. V., Ambaruch, R., 1977, "Remote Sensing Requirements as Suggested by Watershed Model Sensitivity Analyses," Proceedings of the Twelfth International Symposium on Remote Sensing of Environment, ERIM, Michigan.

26. Reeves, R. G., 1975, "Manual of Remote Sensing," The American Society of Photogrammetry.

27. Sasso, R. R., Jensen, J. R., 1977, "Automated Image Processing of LANDSAT II Digital Data for Watershed Runoff Prediction," Proceedings of the Eleventh International Symposium on Remote Sensing of Environment, ERIM, Michigan.

28. Simmons, P. W., 1968, "The Influence of Landuse and Treatment on the Hydrology of Small Watersheds on Coshocton, Ohio," M.S. Thesis, Civil Engineering, The Ohio State University.

29. Silva, L. F., 1978, "Remote Sensing, the Quantitative Approach," Purdue University, McGraw-Hill.

30. Stoner, E. R., Baumgardner, M. F., Cipra, J. E., 1978, "Determining Density of Maize Canopy from Airborne Multispectral Scanner Data," LARS Print 111272, Purdue University.

31. Stoner, E. R., Baumgardner, M. F., Anuta, P. E., Cipra, J. E., 1978, "Determining Density of Maize Canopy by Temporal Analysis," LARS Print 111372, Purdue University.

32. Sinclair, T. R., 1960, "Pathway of Solar Radiates In Through Leaves," M.S. Thesis, Purdue University.

APPENDIX

The Appendix contains several tables and figures providing details related to the analysis and results of the study to establish runoff coefficients from LANDSAT multi-spectral data. The next few paragraphs record regression models used in the classification of the runoff related data.

Several types of models were used in the analysis. The model parameters define the independent variables (channel radiance) that contributed to the shape of the response surface. The procedure follows.

For each training sample (block of 3 x 3 pixels), four independent channel mean variables ($\bar{X}_4$, $\bar{X}_5$, $\bar{X}_6$, $\bar{X}_7$) and one dependent variable CN are selected.

The process is repeated for all the samples until a design matrix of CN versus the four-channel response is constructed for the two LANDSAT scenes. The training samples are shown in Appendix A, Tables 1 and 2.

The CN variables (runoff coefficients) are plotted against each of the channel response values. The plots are shown in Appendix B. The plots provide an insight to the nature of dispersion of the data in the four-dimensional space.

The coefficient of correlation (Appendix C, Tables 1 and 2) between the dependent variable and the independent variables evaluates the significance of each variable. Then, through an iterative process the relationship between radiance values and the runoff coefficient is calculated from regression models having the general form:

$$CN = B_0 + B_1 X_4^{\alpha 1} + B_2 X_5^{\alpha 2} + B_3 X_6^{\alpha 3} + B_4 X_7^{\alpha 4}$$

Appendix C (Tables 1 and 2) presents both data sets for the channels 4, 5, 6 and 7. Most of the channel 4 and 5 variations are better correlated with

the runoff coefficient than the two near-infrared channels 6 and 7. Also, the pairwise correlations between the visible channels 4 and 5, as well as the infrared channels 6 and 7,are very high. From these correlations it is inferred that the dimensionality of the data can be reduced by selecting only the features that contirbute to the relationship. One may also note from the correlation matrices in Appendix C that for the May data (Table 1) the relationship between the runoff coefficient and the two infrared channels are positively correlated, whereas, for the June data the correlation is negative (Table 2). Intuitively, one may speculate that the amount of vegetation foliage, which increased from May 6 to June 20, may be contributing to this relationship. The increase in the foliage results in a higher radiance response in the near infrared channels, at the same time the potential for surface runoff decreases because of more interception by the vegetation.

For each data set a number of linear and polynomial regression models were tested using the SAS statistical package (Barr, 1979)

Finally, the optimum set of exponents and coefficients which produced the highest measure of closeness, R^2 for the model selected showed which regression models fit the runoff coefficients. The best-fit models for both dates are illustrated below. The statistical results and forms that were considered in the analysis appear in Appendix E.

For the May data, the relationship between the channel radiance and the runoff coefficient is better using a polynomial rather than a linear model. The "F" values for each variable in the model are reported in Appendix E, where all the values were significant at the 0.05 level. The classification performance of the models was assessed for the small watersheds of the Little Mill Creek which were used for test site observations on the 1/24000 scale color infrared photography. Considering the analagous and inter-related

physiographic and cultural practices in the area and the visual observations of tonal, textural and color features, it was inferred that the test sites were indeed representative of the entire Mill Creek Watershed.

From the ground truth and the soil region information in Table 1, each test watershed was assigned a weighted CN value. (The results are summarized in Table 3, Appendix D) The boundaries of the test watersheds were manually transferred to an overlay to the spectral maps. From a statistical analysis, the mean radiance values for the test watersheds in the four LANDSAT channels were calculated; Appendix D, Figure 3 gives a typical illustration. The radiance values represent the average spectral response for all land cover condition types within a given test watershed.

The four mean radiance values were supplied to the regression models. The CN values predicted by the models for each test watershed are compared with those obtained from ground truth as shown in Table 1, Appendix F.

Finally, several randomly selected test fields were chosen, and the radiance values were supplied to the models. The results for the performance of the models in predicting the CN value for an individual field (a wood lot, or a field crop) rather than a test watershed are shown in Tables 1 and 2 of Appendix F.

APPENDIX A

List of Training Samples

Table 1 List of the Training Samples for May 6th LANDSAT

Sample Number	Land Cover and Condition	CN Value	Channels $\bar{X}_4$	$\bar{X}_5$	$\bar{X}_6$	$\bar{X}_7$
1	F-C	91	24.66	29.00	40.77	40.11
2	PN1-B	69	23.00	21.33	52.22	63.53
3	F-B	86	28.89	33.66	42.77	40.66
4	WS-B	66	21.22	19.66	39.11	44.66
5	WN-B	60	21.55	20.66	40.88	46.11
6	WS-B	66	21.11	19.55	37.44	41.44
7	WN-B	60	19.88	18.00	33.66	36.66
8	PN1-C	74	28.11	34.11	50.89	54.66
9	WD-B	55	19.33	17.89	30.89	33.33
10	F-B	86	21.33	18.33	51.33	60.77
11	F-B	86	24.44	28.33	43.11	46.55
12	WS-B	66	17.33	17.44	31.11	33.66
13	PN1-C	79	23.55	20.33	61.55	73.66
14	PN1-B	69	25.44	23.44	62.44	73.44
15	PN1-C	79	23.55	19.55	57.55	67.11
16	PN1-C	79	21.89	19.44	52.00	60.55
17	WS-C	77	19.50	18.60	30.10	32.50
18	F-C	91	26.44	31.77	43.44	44.44
19	F-B	86	26.33	32.55	44.44	45.33
20	F-C	91	21.22	19.55	42.77	49.22
21	F-C	91	23.77	25.77	42.11	44.11
22	PN1-B	69	23.11	22.33	54.33	61.77
23	WN-C	73	21.66	20.22	42.44	46.66
24	F-C	91	20.66	18.89	48.66	54.88
25	WD-B	55	20.11	18.00	35.11	38.89
26	WS-C	77	23.00	25.77	40.44	44.55
27	WS-C	77	21.66	23.66	37.33	39.44
28	WN-C	73	20.89	21.33	39.00	44.33
29	F-B	86	24.20	27.30	35.70	34.50
30	F-C	91	22.77	22.55	52.22	59.00
31	F-C	91	23.55	26.44	36.00	37.55
32	F-B	86	25.66	29.22	47.22	47.66
33	WD-C	70	22.50	22.70	36.90	40.10
34	F-C	91	23.55	25.33	35.89	34.55
35	F-C	91	24.89	29.66	46.44	50.11
36	PN1-C	79	22.11	19.11	57.55	69.89
37	PN1-B	69	22.22	20.33	54.88	64.44
38	PN1-B	69	22.44	19.66	56.22	65.22
39	F-C	91	28.11	33.88	52.89	57.55
40	PN1-C	79	24.55	26.00	49.22	53.77
	Average	78	23.05	23.48	45.26	49.93

P = Pasture
W = Woods
F = Fallow fields
N1 = Normal surface condition
D = Dense canopy
S = Sparse canopy
N = Normal canopy
B = Hydrologic soil group
C = Hydrologic soil group

Table 2 List of the Training Samples for June 20th LANDSAT

Sample Number	Land Cover and Condition	CN Value	Channels $\bar{X}_4$	$\bar{X}_5$	$\bar{X}_6$	$\bar{X}_7$
1	RCR-B	80	34.25	43.62	65.87	56.37
2	WD-C	70	19.77	16.44	51.55	51.00
3	RCR-B	80	24.66	28.00	55.00	49.33
4	WN-C	73	20.66	17.66	60.89	64.33
5	RCT-C	79	27.33	33.55	57.66	52.33
6	RCT-C	79	25.75	28.25	58.62	56.00
7	RCT-B	73	26.77	31.89	58.00	53.55
8	PN-B	69	24.25	23.16	62.66	62.73
9	PN-B	69	22.00	21.14	54.85	56.00
10	WS-C	77	22.77	21.11	64.89	68.66
11	RCR-B	80	32.70	41.00	60.50	50.99
12	WS-C	77	21.00	17.20	62.90	67.50
13	RCC-C	83	23.44	22.77	61.70	60.00
14	PN-C	79	22.89	19.77	59.66	59.22
15	WN-C	73	20.72	17.45	68.27	74.54
16	PN-C	79	23.00	21.75	53.83	51.75
17	RCC-B	77	25.89	27.22	57.33	53.33
18	PN-B	69	21.41	19.00	56.58	58.16
19	WS-C	77	19.89	15.22	60.55	65.33
20	RCR-B	80	25.55	26.66	55.11	53.33
21	WN-C	73	19.66	16.78	61.00	65.66
22	WS-C	77	18.33	16.11	65.77	69.55
23	WN-C	73	19.60	16.10	62.40	65.80
24	RCC-C	83	24.11	24.44	55.89	53.00
25	PN-B	69	18.44	16.77	60.22	64.22
26	WD-C	70	23.22	21.89	59.77	59.89
27	PN-C	79	20.50	17.33	58.16	59.33
28	PN-C	79	21.11	19.33	65.11	63.00
29	RCC-C	83	28.33	32.55	59.33	53.55
30	RCR-B	80	19.44	17.33	59.22	61.77
31	RCC-B	77	24.33	27.77	52.44	47.55
32	RCT-C	79	25.00	28.66	55.00	51.44
33	RCT-C	79	28.11	34.55	58.22	51.66
34	PN-C	79	21.66	22.11	53.22	50.89
35	RCR-B	80	25.60	28.20	56.90	53.30
36	PN-B	69	22.90	21.10	62.40	63.40
37	RCC-C	83	28.22	34.22	57.66	52.55
38	RCR-B	80	22.33	21.22	55.89	53.44
39	RCR-B	80	19.89	18.55	58.55	60.11
40	RCR-B	80	21.50	19.50	59.49	59.70
41	WS-B	66	19.00	16.33	63.00	66.44
42	RCR-B	80	27.79	33.80	54.60	48.70
43	RCR-B	80	29.11	35.77	57.33	49.11
44	WN-C	73	23.11	25.11	50.66	46.44
45	WS-B	66	19.77	17.77	56.77	59.44
46	RCR-B	80	28.55	34.55	58.00	50.88
47	Roads	90	29.22	36.33	58.55	52.89
48	WN-C	73	19.00	17.20	60.10	63.80
	Average	76.73	23.59	24.26	58.79	57.54

Table 2 Continued

RCC = Row Crop Contoured
RCR = Row Crop Straight Row
RCT = Row Crop Contoured and Terraced
W = Woods
P = Pasture
S = Sparse Canopy
N = Normal Canopy
D = Dense Canopy
N1 = Normal Surface Condition
B = Hydrologic Soil Group
C = Hydrologic Soil Group

APPENDIX B

Plots of CN Values vs. Channel Radiance Responses

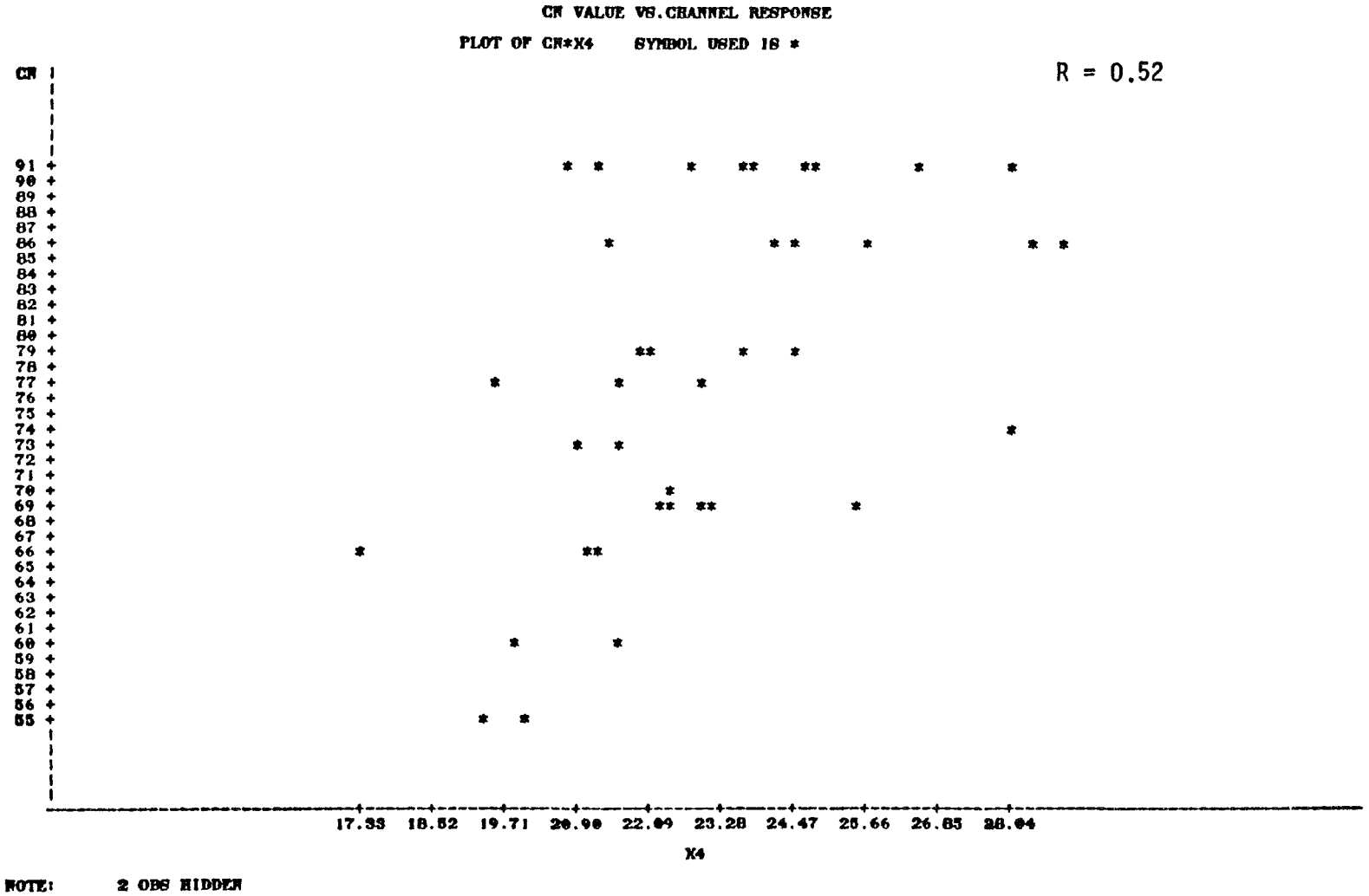

Figure 1 Plot of CN Value vs. Channel 4 Response for May Data

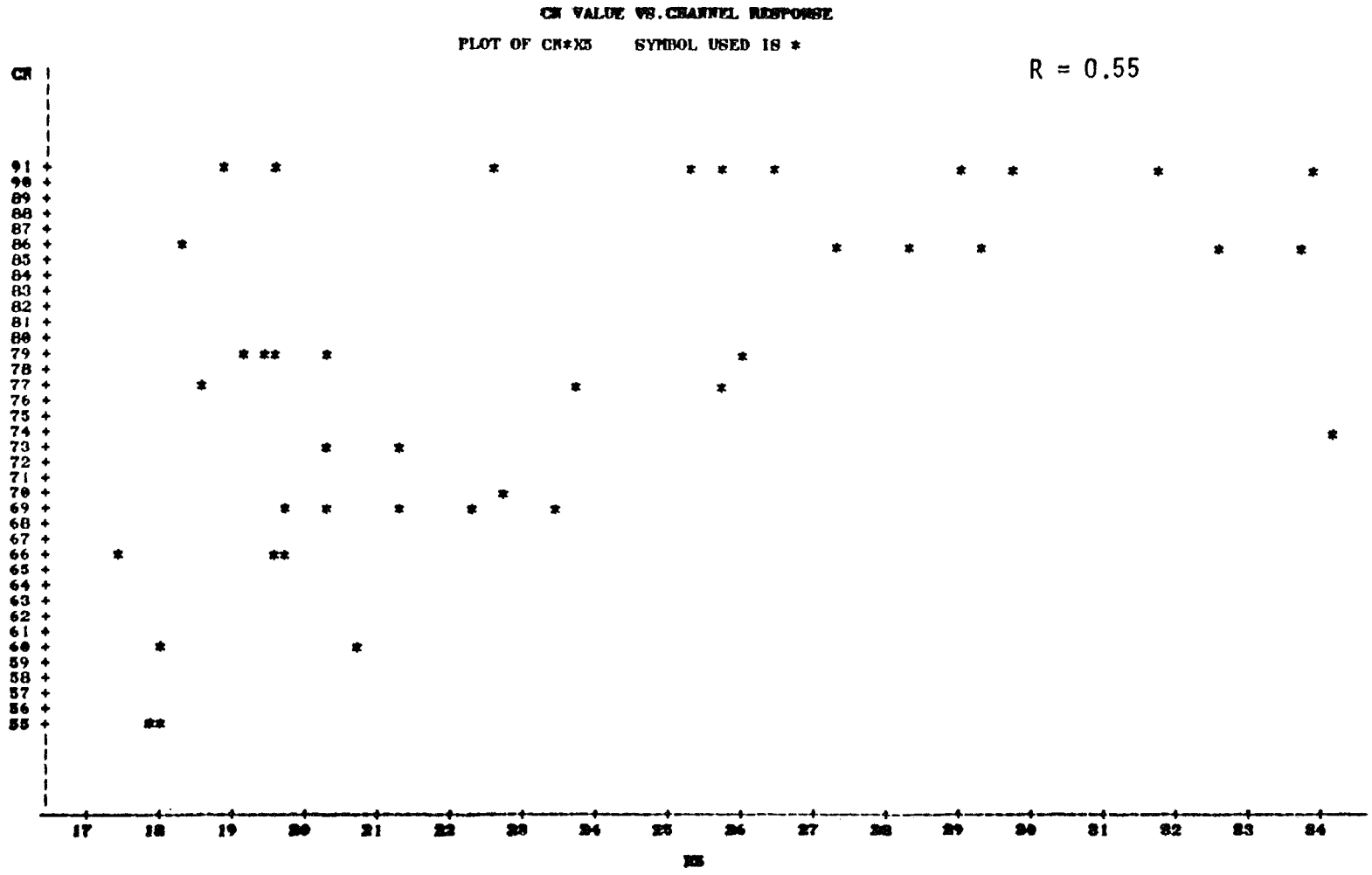

Figure 2 Plot of CN Value vs. Channel 5 Radiance Response for May Data

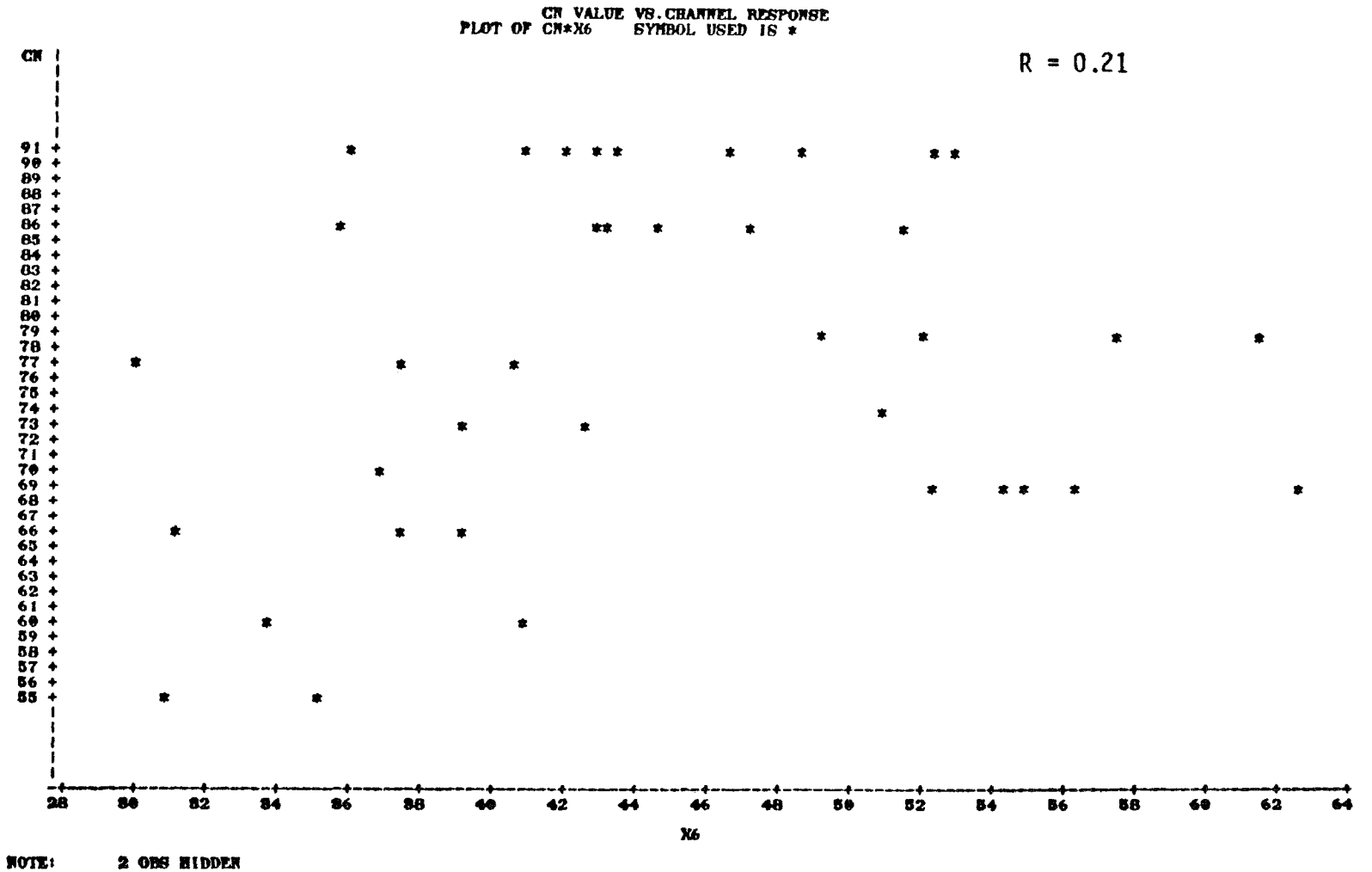

Figure 3 Plot of CN Value vs. Channel 6 Radiance Response for May Data

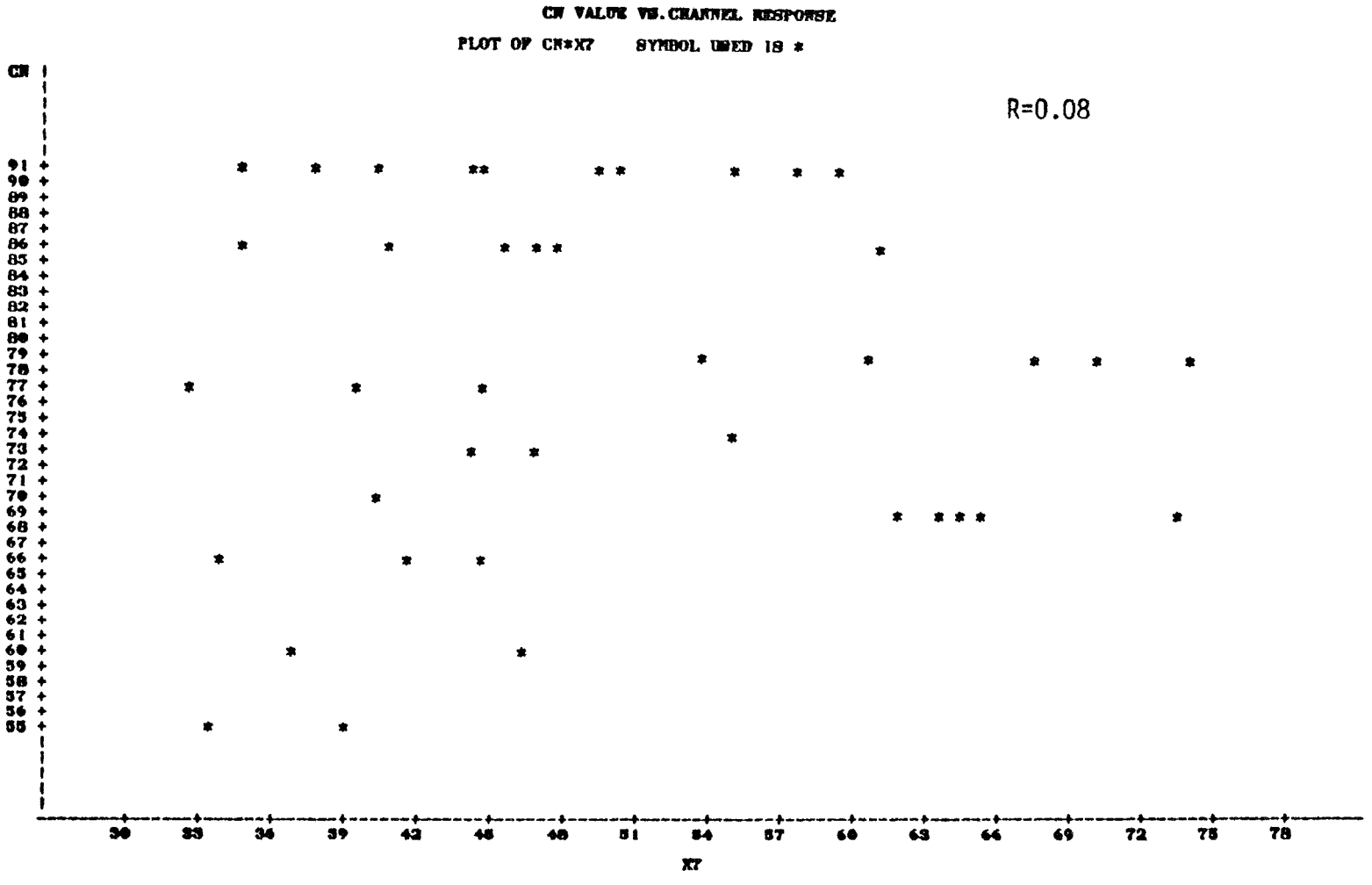

Figure 4 Plot of CN Value vs. Channel 7 Radiance Response for May Data

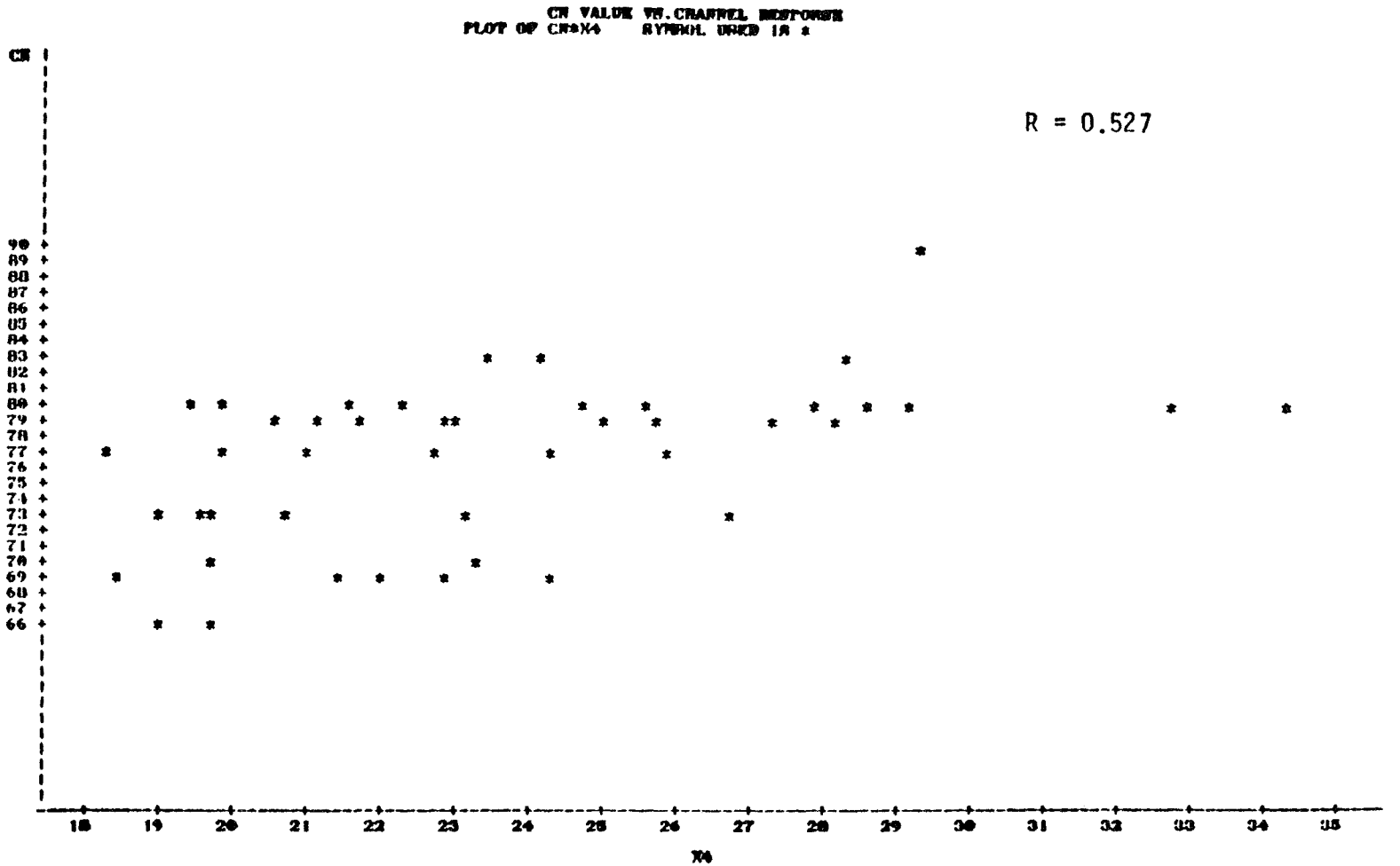

Figure 5 Plot of CN Value vs. Channel 4 Radiance Response for June Data

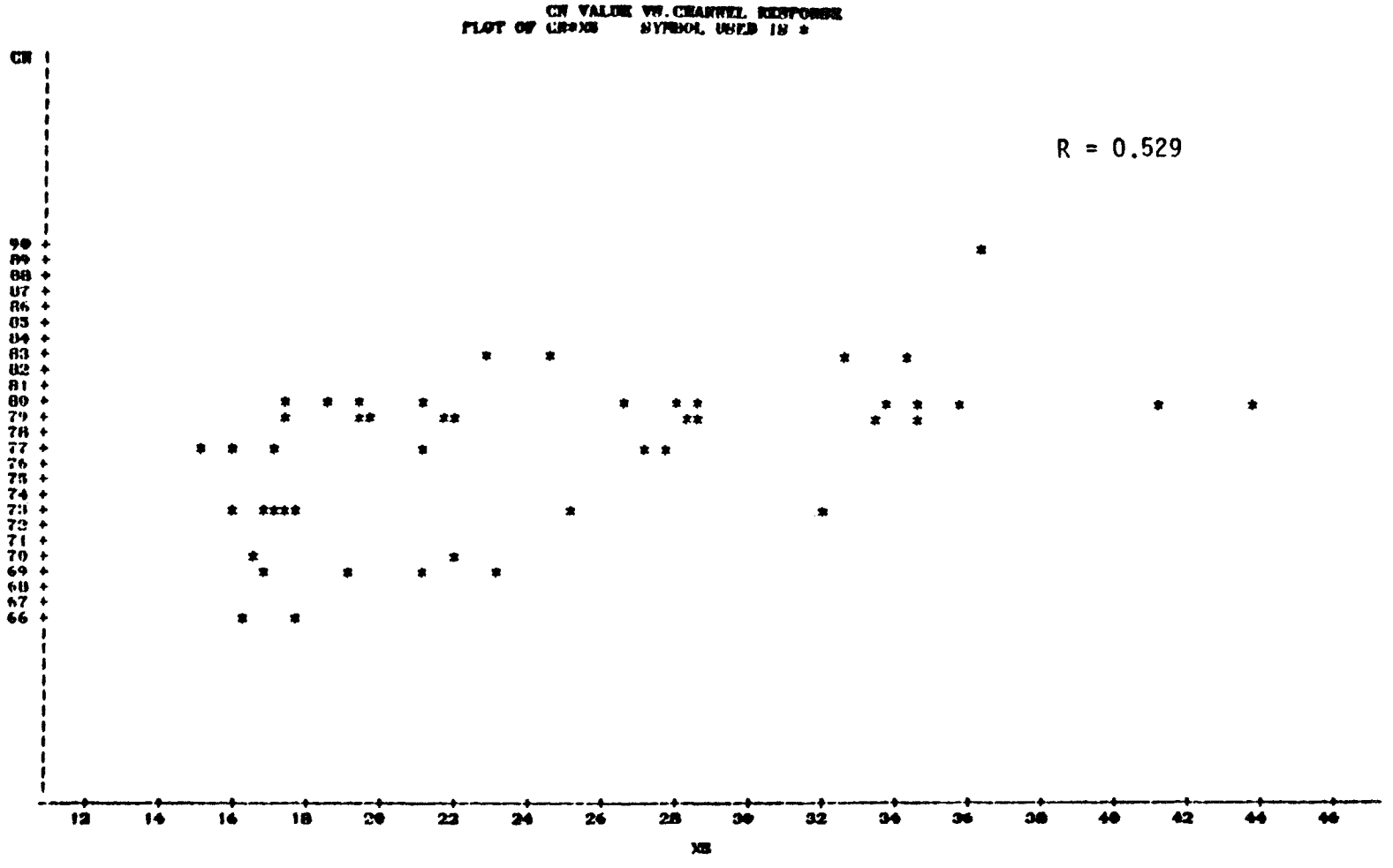

Figure 6. Plot of CN Value vs. Channel 5 Radiance Response for June Data

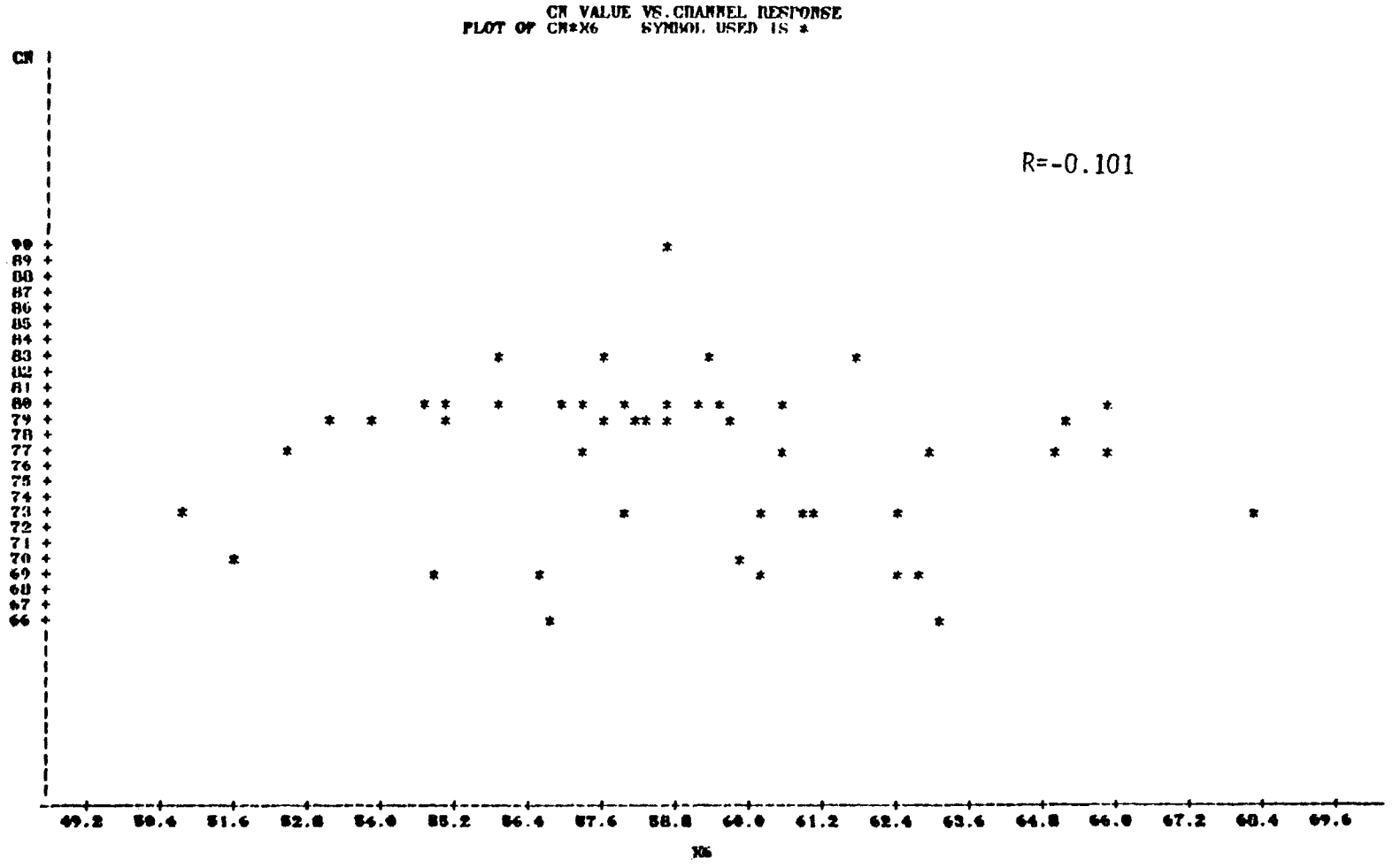

Figure 7 Plot of CN Value vs. Channel 6 Radiance Response for June Data

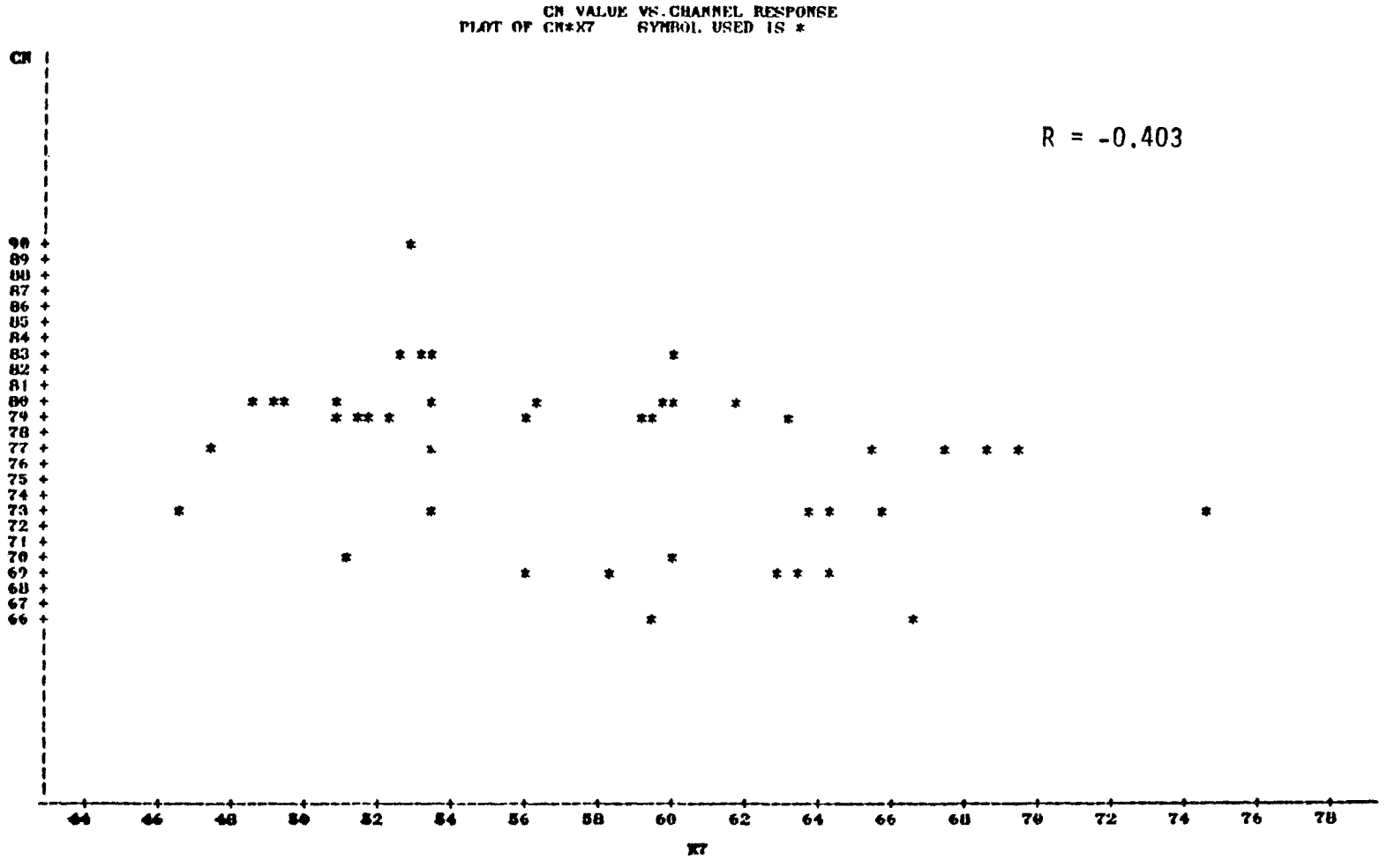

Figure 8 Plot of CN Value vs. Channel 7 Radiance Response for June Data

APPENDIX C

Results of Statistical Analysis

Table 1 Results of the Statistical Analysis Generated for the May 6th Data

Mean value for CN obtained from 41 observations = 78

standard deviation = 10.96

Variance - Covariance Matrix

The matrix for the independent variables is a square matrix of size 4 X 4.

$$\begin{bmatrix} S_4^2 & S_{45} & S_{46} & S_{47} \\ S_{54} & S_5^2 & S_{56} & S_{57} \\ S_{64} & S_{65} & S_6^2 & S_{67} \\ S_{74} & S_{75} & S_{76} & S_7^2 \end{bmatrix} = \begin{bmatrix} 6.53 & 11.68 & 8.76 & 6.57 \\ 11.68 & 25.21 & 1.93 & -7.81 \\ 8.75 & 1.93 & 85.61 & 108.86 \\ 6.57 & -7.81 & 108.86 & 146.19 \end{bmatrix}$$

$(Si)^2$ = variance

Sij = covariance between two channels.

Correlation Coefficient Matrix

The 5 X 5 matrix defines the correlation coefficient between the channels, and the department variables.

	CN	X_4	X_5	X_6	X_7
CN	1.0				
X_4	0.52	1.0			
X_5	0.55	0.91	1.0		
X_6	0.21	0.37	0.04	1.0	
X_7	0.08	0.21	-0.13	0.97	1.0

Table 2 Results of the Statistical Analysis Generated for the June 20th Data

Mean value for CN obtained from 48 observations = 77

standard deviation = 5.10

Variance - Covariance Matrix

The matrix for the independent variables is a square matrix of size 4 X 4.

$$\begin{bmatrix} S_4^2 & S_{45} & S_{46} & S_{47} \\ S_{54} & S_5^2 & S_{56} & S_{57} \\ S_{64} & S_{65} & S_6^2 & S_{67} \\ S_{74} & S_{75} & S_{76} & S_7^2 \end{bmatrix} = \begin{bmatrix} 14.29 & 27.64 & -1.70 & -15.85 \\ 27.64 & 55.53 & -5.19 & -33.84 \\ -1.70 & -5.19 & 14.90 & 21.32 \\ -15.86 & -33.04 & 21.32 & 45.18 \end{bmatrix}$$

$(S_i)^2$ = variance

S_{ij} = covariance between two channels

Correlation Coefficient Matrix

The 5 X 5 matrix defines the correlation coefficient between the channels, and the dependent variable.

	CN	X_4	X_5	X_6	X_7
CN	1.0				
X_4	0.527	1.0			
X_5	0.529	0.98	1.0		
X_6	-0.101	-0.116	-0.18	1.0	
X_7	-0.403	-0.624	-0.675	0.821	1.0

APPENDIX D

Ground Truth Data

Table 1 Ground Truth Corresponding to June Data

Watershed test number	Percent Area of Land Cover-Surface Condition								Weighted CN
	RCR	RCC	RCT	WS	WN	WD	PN	F	
5	19	18	0	0	38	0	5	20	77
9	0	0	0	12	66	0	22	0	73
10	48	0	28	24	0	0	0	0	82
11	0	2	21	11	30	0	12	5	77
13	0	0	0	85	0	0	12	3	68
20	0	25	0	15	16	0	44	0	78
91	66	6	0	25	0	3	0	0	81
92	30	6	0	45	9	0	11	0	75
94	14	41	10	5	30	0	0	0	73
95	26	34	0	0	9	0	17	0	75
97-A	6	16	26	18	5	3	26	0	76

Key to the table:

RCR = Row crop straight row

RCC = Row crop contoured

RCT = Row crop contoured and terraced

WS = Woods sparse canopy

WN = Woond normal canopy

WD = Woods dense canopy

PN = Pasture

F = Fallow

Table 2 Mean Radiance for Test Watersheds, June Data

Test Watershed Number	Mean Radiance Response and (standard deviation) for Channels			
	X_4	X_5	X_6	X_7
5	23.95	22.60	66.90	69.00
	(2.96)	(5.39)	(4.09)	(7.70)
9	23.33	21.23	68.22	71.15
	(2.94)	(4.93)	(5.19)	(7.29)
10	27.93	29.54	63.44	60.51
	(3.35)	(6.23)	(3.67)	(6.18)
11	26.18	26.25	66.25	65.64
	(3.41)	(4.56)	(4.27)	(5.86)
13	22.91	20.62	63.77	65.61
	(2.59)	(4.28)	(4.43)	(5.43)
20	24.07	22.01	66.07	66.98
	(3.49)	(4.58)	(8.79)	(10.30)
91	23.32	22.15	64.00	64.72
	(5.10)	(7.04)	(11.46)	(12.04)
92	25.61	25.75	65.48	65.62
	(4.09)	(7.56)	(4.04)	(7.37)
94	25.17	24.60	65.60	65.90
	(3.26)	(5.68)	(4.21)	(6.49)
95	25.64	25.21	64.00	63.22
	(2.30)	(4.17)	(4.07)	(5.40)
97-A	25.16	24.00	65.24	65.37
	(3.30)	(3.74)	(5.87)	(7.01)

APPENDIX E

Regression Models

Table 1 Regressions Models for May Data

$$CN = B_0 + B_1 X_4^{\alpha 1} + B_2 X_5^{\alpha 2} + B_3 X_6^{\alpha 3} \quad B_4 X_7^{\alpha 4}$$

CN = runoff coefficient

X_4 = the mean radiance in Channel 4 of LANDSAT data

X_5 = the mean radiance in Channel 5 of LANDSAT data

X_6 = the mean radiance in Channel 6 of LANDSAT data

X_7 = the mean radiance in Channel 7 of LANDSAT data

Model 1

$$CN = 70.16 - 3.76\ X_4 + 1.97\ X_5 + 3.50\ X_6 - 2.20\ X_7$$

Variable	F value	Significant level
X_4	2.54	0.12
X_5	3.03	0.09
X_6	4.67	0.04
X_7	3.61	0.06

(R^2) for the model = 0.43

Model 2

$$CN = 13.71 - 4.70\ X_4 + 54.61\ X_5^{1/3} - 2308.9\ X_6^{-1/2} + 1330.3\ X_7^{-1/3}$$

Variable	F value	Significant level
X_4	5.29	0.03
$X_5^{1/3}$	5.20	0.03
$\frac{1}{(X_6)^{1/3}}$	9.84	0.003
$\frac{1}{(X_7)^{1/2}}$	7.63	0.009

(R^2) for the model = 0.51

Table 2 Regression Models for June Data

$$CN = B_0 + B_1 X_4^{\alpha 1} + B_2 X_5^{\alpha 2} + B_3 X_6^{\alpha 3} + B_4 X_7^{\alpha 4}$$

CN = runoff coefficient

X_4 = the mean radiance in Channel 4 of LANDSAT data

X_5 = the mean radiance in Channel 5 of LANDSAT data

X_6 = the mean radiance in Channel 6 of LANDSAT data

X_7 = the mean radiance in Channel 7 of LANDSAT data

Model 3

$CN = 63.56 + 0.126X_4 - 0.166\ X_5 + 1.04\ X_6 - 0.84\ X_7$

Variable	F value	Significance level
X_4	0.02	0.89
X_5	0.05	0.82
X_6	2.48	0.12
X_7	2.82	0.10

(R^2) for the model = 0.32

Model 4

$CN = 72.56 + 0.32\ X_5 - 0.06\ X_7$

Variable	F value	Significance level
X_5	7.62	0.008
X_6	0.24	0.62

(R^2) for the model = 0.28

Table 2 Continued

Model 5

$$CN = 49.17 + 0.24\ X_4 - 0.23\ X_5 - 1068.6\ X_6^{-\frac{1}{2}} + 643.0\ X_7^{-1/3}$$

Variable	F value	Significance level
X_4	.03	0.87
X_5	.04	0.83
$\frac{1}{(X_6)^{\frac{1}{2}}}$	2.61	0.11
$\frac{1}{(X_7)^{1/3}}$	2.73	0.11

(R^2) for the model = 0.33

APPENDIX F

Performance of Regression Models

Table 1 Performance of Regression Models in Predicting CN Values, May Data

Test Fields	CN Obtained From Ground Truth	CN Predicted by: Model 1	Model 2
F-C	91	89	97
WS-B	66	68	72
WS-C	77	78	84
F-B	86	72	78
WD-B	55	67	70
WN-C	73	73	78
WD-C	70	71	76
PN1-C	79	72	79
PN1-B	69	78	83

F = Fallow fields

W = Woods

P = Pasture

N1 = Normal surface condition

S = Sparse canopy

N = Normal canopy

D = Dense canopy

B - Hydrologic soil group

C = Hydrologic soil group

Table 2 Performance of Regression Models in Predicting CN Values, June Data

Test Fields	CN Obtained From Ground Truth	CN Predicted by: Model 3	Model 4	Model 5
RCR-B	80	84	83	84
WN-C	73	73	74	73
WS-B	66	74	74	73
RCT-C	79	81	81	81
RCC-B	77	78	79	79
PN1-B	69	73	74	73
RCC-C	83	80	80	81
WD-C	70	76	76	76
PN1-C	79	77	76	77

RCR - Row crop straight row

RCC = Row crop contoured

RCT = Row crop contoured and terraced

W = Woods

N = Normal canopy

S = Sparse canopy

D = Dense canopy

N1 = Normal surface condition

C = Hydrologic soil group

B = Hydrologic soil group

Table 3 Performance of Regression Models in Predicting the Weighted CN Values, June Data

Test Watershed Number	Weighted CN Obtained From Ground Truth	Mean CN Predicted by:		
		Model 3	Model 4	Model 5
5	77	76	76	78
9	73	75	75	78
10	82	79	78	81
11	77	78	77	80
13	68	75	75	78
20	78	77	76	79
91	81	76	76	79
92	75	77	77	79
94	73	77	76	79
95	75	78	77	80
97A	76	77	76	77

APPENDIX G

Spectral Map and Radiance Histograms

MAP

STATISTICAL INFORMATION FOR CATEGORY 1, SAMPLE 1 TRAINING AREA

NUMBER OF OBSERVATIONS: 275

UNNORMALIZED DATA USED

CLASS 5.26

CHANNELS USED : 1 2 3 4

MEANS AND STANDARD DEVIATIONS FOR GIVEN CHANNELS

CHANNEL	1	2	3	4
MEAN	25.64	25.21	64.00	63.22
ST. DEV.	2.30	4.17	4.07	5.40

VARIANCE-COVARIANCE MATRIX

	1	2	3	4
1	5.29			
2	8.16	17.41		
3	1.19	0.12	16.53	
4	-3.25	-9.31	17.27	29.15

CORRELATION MATRIX FOR GIVEN CHANNELS

	1	2	3	4
1	1.00			
2	0.25	1.00		
3	0.13	0.01	1.00	
4	-0.26	-0.41	0.79	1.00

Figure 1 Spectral Map for Test Watershed 95

HISTOGRAM FOR CHANNEL 1 0.50 - 0.60 MICRONS.

EACH * REPRESENTS 1 OBSERVATION(S).

FREQUENCY	GREY LEVEL	
1	19	I*
2	20	I**
6	21	I*****
16	22	I****************
21	23	I*********************
44	24	I**
45	25	I***
49	26	I**
30	27	I******************************
29	28	I*****************************
17	29	I*****************
14	30	I**************
2	31	I**

HISTOGRAM FOR CHANNEL 2 0.60 - 0.70 MICRONS.

EACH * REPRESENTS 1 OBSERVATION(S).

FREQUENCY	GREY LEVEL	
10	18	I**********
5	19	I*****
25	20	I************************
14	21	I**************
17	22	I*****************
30	23	I******************************
39	24	I**************************************
16	25	I****************
25	26	I************************
15	27	I***************
16	28	I****************
19	29	I******************
17	30	I*****************
7	31	I*******
4	32	I****
7	33	I*******
4	34	I****
	35	I
1	36	I*
1	37	I*
3	38	I***

HISTOGRAM FOR CHANNEL 3 0.70 - 0.80 MICRONS.

EACH * REPRESENTS 1 OBSERVATION(S).

FREQUENCY	GREY LEVEL	
1	53	I*
1	54	I*
	55	I
9	56	I*********
8	57	I********
7	58	I*******
16	59	I****************
15	60	I***************
21	61	I*********************
17	62	I*****************
29	63	I*****************************
17	64	I*****************
29	65	I*****************************
25	66	I************************
30	67	I******************************
12	68	I************
11	69	I***********
13	70	I*************
8	71	I********
4	72	I****
1	73	I*
1	74	I*

HISTOGRAM FOR CHANNEL 4 0.80 - 1.10 MICRONS.

EACH * REPRESENTS 1 OBSERVATION(S).

FREQUENCY	GREY LEVEL	
1	46	I*
	47	I
	48	I
	49	I
1	50	I*
1	51	I*
3	52	I***
2	53	I**
4	54	I****
7	55	I*******
4	56	I****
12	57	I************
16	58	I****************
18	59	I******************
28	60	I****************************
15	61	I***************
17	62	I*****************
19	63	I*******************
15	64	I***************
18	65	I******************
16	66	I****************
21	67	I*********************
13	68	I*************
7	69	I*******
7	70	I*******
11	71	I***********
4	72	I****
7	73	I*******
1	74	I*
4	75	I****
3	76	I***

Figure 2 Radiance Histograms for Test Watershed 95